Strong correlations and spin-density-wave phase induced by a massive spectral weight redistribution in alpha-Fe1.06Te

Y. Zhang, F. Chen, C. He, L. X. Yang, B. P. Xie, Y. L. Xie, X. H. Chen, M. Fang, M. Arita, K. Shimada, H. Namatame, M. Taniguchi, J. P. Hu, and D. L. Feng

Strong correlations and spin-density-wave phase induced by a massive spectral weight redistribution in α-$Fe_{1.06}Te$

Y. Zhang,[1] F. Chen,[1] C. He,[1] L. X. Yang,[1] B. P. Xie,[1] Y. L. Xie,[2] X. H. Chen,[2] Minghu Fang,[3] M. Arita,[4] K. Shimada,[4] H. Namatame,[4] M. Taniguchi,[4] J. P. Hu,[5] and D. L. Feng[1,*]

[1]*State Key Laboratory of Surface Physics, Department of Physics, Advanced Materials Laboratory, Fudan University, Shanghai 200433, People's Republic of China*

[2]*Department of Physics, University of Science and Technology of China, Hefei, Anhui 230027, People's Republic of China*

[3]*Department of Physics, Zhejiang University, Hangzhou 310027, China*

[4]*Hiroshima Synchrotron Radiation Center and Graduate School of Science, Hiroshima University, Hiroshima 739-8526, Japan*

[5]*Department of Physics, Purdue University, West Lafayette, Indiana 47907, USA*

(Received 21 September 2010; revised manuscript received 24 September 2010; published 13 October 2010)

The electronic structure of α-$Fe_{1.06}Te$ is studied with angle-resolved photoemission spectroscopy. We show that there is substantial spectral weight around Γ and X, and line shapes are intrinsically broad in the paramagnetic state. The magnetic transition is characterized by a massive spectral weight transfer over an energy range as large as the bandwidth, which even exhibits a hysteresis loop that marks the strong first-order transition. Coherent quasiparticles emerge in the magnetically ordered state due to decreased spin fluctuations, which accounts for the change in transport properties from insulating behavior to metallic behavior. Our observation demonstrates that $Fe_{1.06}Te$ distinguishes itself from other iron-based systems with more local characters and much stronger interactions, and how a spin-density wave is formed in the presence of strong correlation.

DOI: 10.1103/PhysRevB.82.165113 PACS number(s): 74.25.Jb, 71.20.−b, 74.70.Xa, 79.60.−i

I. INTRODUCTION

The discovery of iron-based high-temperature superconductors (Fe-HTSCs) has generated great interests.[1] So far, two classes of Fe-HTSC have been discovered. They are iron pnictides, e.g., $SmO_{1-x}F_xFeAs$ or $Ba_{1-x}K_xFe_2As_2$,[2,3] and iron chalcogenides, e.g., $Fe_{1+y}Te_{1-x}Se_x$.[4,5] Although, both classes of materials share many common aspects, such as similarly high maximal superconducting transition temperature (T_c) [$Fe_{1+y}Se$ possesses a T_c of 37 K under hydrostatic pressure of 7 GPa (Ref. 6)] and similar band structures from density-functional theory (DFT) calculations.[7,8] However, their parent compounds exhibit quite different spin-density wave (SDW) states. A collinear commensurate antiferromagnetic order has been identified for the pnictides,[9,10] while a bicollinear and 45° rotated antiferromagnetic order was identified for $Fe_{1+y}Te$.[11,12] Furthermore, the transport properties of $Fe_{1+y}Te$ respond abruptly to the first-order magnetic/structural transition. In the paramagnetic state, it shows insulatorlike resistivity [Fig. 1(e)], and optical conductivity without a Drude peak while the resistivity becomes metalliclike, and a Drude peak emerges in the SDW state.[13,14]

Like the cuprates, the nature of magnetic order and spin fluctuations in Fe-HTSC are most likely crucial for its superconductivity. Yet the origin of the magnetic ordering in iron pnictides/chacogenides is still under heated debate. For the iron pnictides, previous studies have shown that the large reconstruction of the band structure dominates the savings of electronic energy, and would be responsible for the SDW (Refs. 15–18) while there are also suggestions that the SDW might be dominated by Fermi-surface nesting.[19] For the iron chalcogenides, a connection between the electronic structure and the bicollinear magnetic structure has not been established, except that Fermi-surface nesting has been ruled out.[13,20] Many fundamental questions are yet to be addressed for iron chalcogenides: why are they different from the iron pnictides; what is responsible for the anomalous transport behaviors in iron chalcogenides? The answers of these questions will help build a general picture of iron-based superconductors.

In this paper, we study the electronic structure of a prototypical parent iron chalcogenide, α-$Fe_{1.06}Te$, by angle-resolved photoemission spectroscopy (ARPES). We found that it is profoundly different from those of iron pnictides. The electronic structure of $Fe_{1.06}Te$ is dominated by strong correlation, which induces broad spectra over extended momentum region in the paramagnetic state. A large square shape of spectral weight unexpectedly appear around Γ and extend to X near the Fermi energy (E_F). In the SDW state, with the spectral weight redistribution over a large energy scale of 0.7 eV, sharp quasiparticle peaks emerge near E_F, indicating reduced spin fluctuations. Through detailed temperature-dependent studies, we show that the massive redistribution of the spectral weight could be responsible for the magnetic transition, unveiling a unique manifestation of SDW on electronic structure in the presence of strong correlation.

II. MATERIAL AND EXPERIMENTAL SETUP

α-$Fe_{1.06}Te$ single crystals were synthesized following the method in Ref. 21. Magnetic-susceptibility measurements show that the SDW transition occurs at T_s=70 K, accompanied by a structural transition, which is consistent with the neutron and transport reports.[12,13] ARPES data were taken with circularly polarized 24 eV photon at the Beamline 9 of Hiroshima synchrotron radiation center (HiSOR) with a Scienta R4000 electron analyzer. The energy resolution is 10

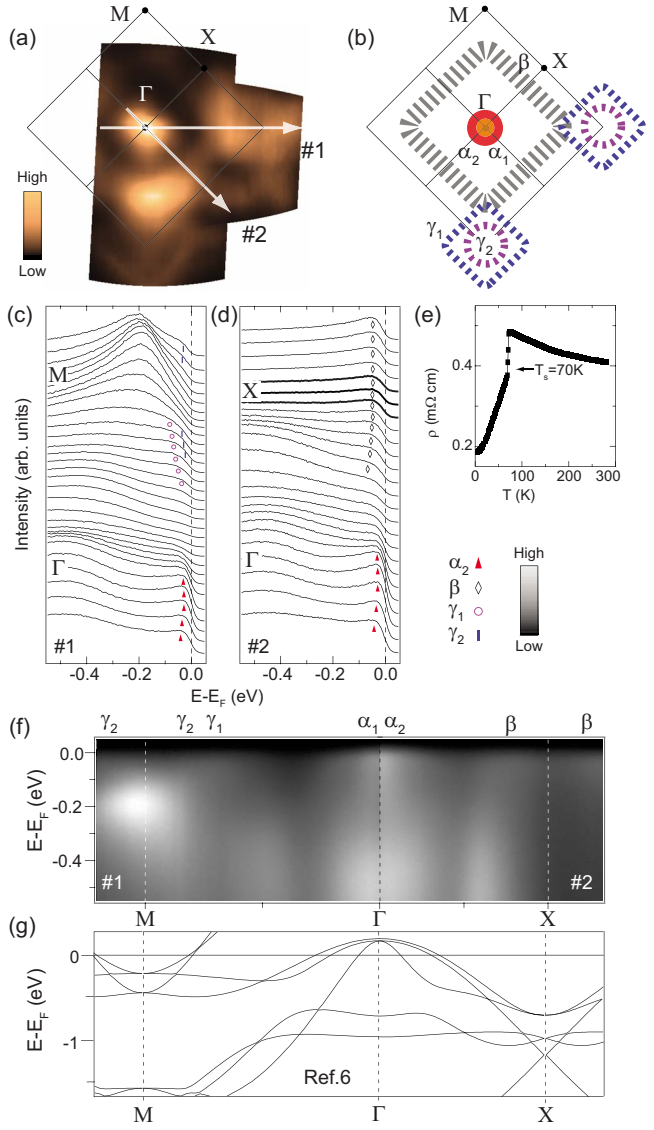

FIG. 1. (Color online) Paramagnetic state electronic structure of $Fe_{1.06}Te$ measured at 135 K. (a) Photoemission intensity distribution integrated over the energy window of $[E_F-15$ meV$,E_F+15$ meV$]$. (b) The spectral weight distribution around E_F, which are labeled by the small filled orange circle (α_1), the large filled red circle (α_2), the dashed black square (β), the large dashed blue squares (γ_1), and small dashed purple squares (γ_2). (c) and (d) The EDCs along cut #1 and #2, respectively. (e) The temperature dependence of the resistivity of $Fe_{1.06}Te$. (f) The photoemission intensities along the M-Γ-X high-symmetry lines, and (g) the corresponding band structure based on DFT calculations (Ref. 7).

meV and angular resolution is 0.3°. The sample was cleaved *in situ*, and measured under ultrahigh vacuum of 3×10^{-11} torr. Aging effects are strictly monitored during the experiments.

III. RESULTS AND DISCUSSIONS

The electronic structure of $Fe_{1.06}Te$ in the paramagnetic state is shown in Fig. 1. The spectra are characterized by a very broad feature. The Fermi crossings are not well defined, analogous to the pseudogap in the cuprates. According to the spectral weight distribution near E_F [Figs. 1(a), 1(c), 1(d), and 1(f)], five main features are labeled as $\alpha_{1,2}$, β, and $\gamma_{1,2}$. Their weight distribution is sketched in Fig. 1(b). Note that, α_1 contributes a straight dispersed feature at Γ, thus it could not be recognized from energy distribution curves (EDCs). The features near E_F around Γ and M qualitatively agree with calculations after renormalized by a factor of about 3 as illustrated by the different energy scales of Figs. 1(f) and 1(g). Thus, the spectral weight of $\alpha_{1,2}$ and $\gamma_{1,2}$ might be attributed to the hole and electron pockets respectively, as in $Fe_{1+y}Te_xSe_{1-x}$.[22] However, contradicting to the calculations, a fair amount of spectral weight around X could be observed near E_F in Fig. 1(d), i.e., the extended β feature.

Many changes occur in the SDW state electronic structure (Fig. 2). Most notably, a dramatic reorganization of the spectral weight is observed in Fig. 2(a), where the weight suppression around X is particularly strong. Such suppression is obvious by comparing the EDCs around X (thick curves) in Figs. 1(d) and 2(c). Similar to $BaFe_2As_2$, the SDW state of $Fe_{1.06}Te$ is accompanied by band shifts. As shown by momentum distribution curves (MDCs) in Fig. 2(d), the distance between two α_2 peaks decreases in the SDW state, indicating a change in dispersion below T_s. The γ_1 and γ_2 bands also exhibit an abrupt momentum shift below T_s, illustrating the enlargement of the electron pockets and band movement around M [Fig. 2(e)]. More remarkably, sharp peaks appear at E_F around Γ and X in Figs. 2(b) and 2(c), forming a peak-dip-hump structure, where the sharp peak and the broad hump could be considered as the coherent and incoherent part of the single-particle spectrum, respectively.[23,24] Both the flat dispersion and the low spectral weight of the coherent quasiparticle peaks suggest a small renormalization factor Z, indicating the existence of strong coupling among electrons and bosonic modes such as spin fluctuations or phonons.[23,24] The formation of sharp coherent quasiparticle peaks with clear Fermi edges naturally explain the metallic resistivity and Drude peak in optical conductivity in the SDW state.[13] On the other hand, when the spectral weight of the coherent quasiparticles disappear in the paramagnetic state, the spectra are dominated by incoherent features as shown in Figs. 1(c) and 1(d). The width of the peaks in the spectra, representing the scattering rate, is significantly larger than its energy distance to the E_F, which results in pseudogaplike line shape. This is consistent with the insulating behavior and the absence of Drude peak in optical conductivity.[13]

Due to the low weight of the coherent quasiparticles, and broad overall line shape, the dominating effect on the electronic structure is not the band shift but the substantial spectral weight redistribution over a large energy scale. Figure 3(a) plots the difference between the integrated spectral weight over $[E_F-0.7$ eV$,E_F+0.05$ eV$]$ at 135 and 15 K in the Brillouin zone. It is clear that spectral weight is suppressed over extended momentum region, and enhanced around Γ at low temperature. Figures 3(b)–3(d) compare the EDCs at various representative momenta in the paramagnetic and SDW states. The enhancement of spectral weight often happens within $[E_F-0.7$ eV$,E_F-0.2$ eV$]$ while the suppression often occurs within $[E_F-0.4$ eV$,E_F]$. We note that

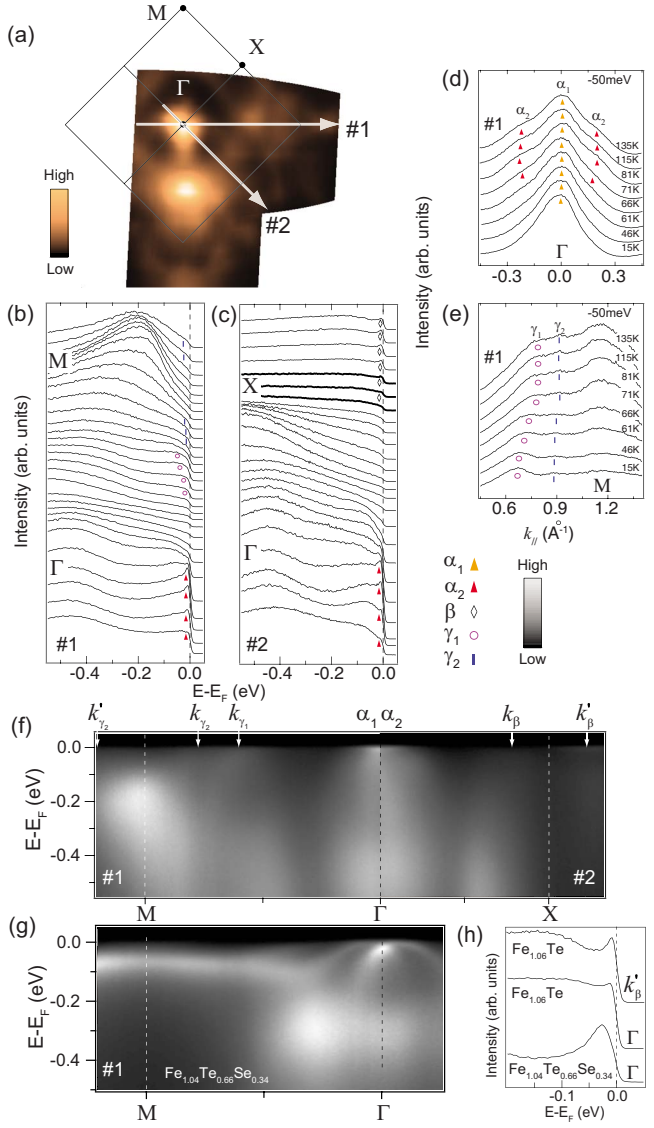

FIG. 2. (Color online) SDW state electronic structure of $Fe_{1.06}Te$ measured at 15 K. (a) Photoemission intensity distribution integrated over the energy window of $[E_F-15\ \text{meV}, E_F+15\ \text{meV}]$. (b) and (c) The EDCs along cut #1 and cut #2, respectively. (d) and (e) are MDCs at −50 meV around Γ and M at different temperatures, respectively. (f) The photoemission intensities along the M-Γ-X high-symmetry lines. Various Fermi crossings are denoted by the short arrows. (g) The photoemission intensity of $Fe_{1.04}$ ($Te_{0.66}Se_{0.34}$) along M-Γ. (h) The EDCs taken at 15 K for $Fe_{1.04}(Te_{0.66}Se_{0.34})$ at Γ, and for $Fe_{1.06}Te$ at Γ and k'_β.

due to the matrix element effects, which are distinct for different bands and momenta, the difference map is not entirely symmetric. For example, the high-energy part in EDC at momentum 4 is more prominent than that at momentum 3 while the EDCs at momenta 2 and 5 look similar. Overall, a large amount of spectral weight is transferred from lower binding energies to higher binding energies, as a result, the electronic energy is significantly reduced. From electronic-structure perspective, it thus could drive the SDW. Such a suppression over a large energy scale is not relevant to Fermi-surface instabilities such as nesting. Consistently, no sign of gap

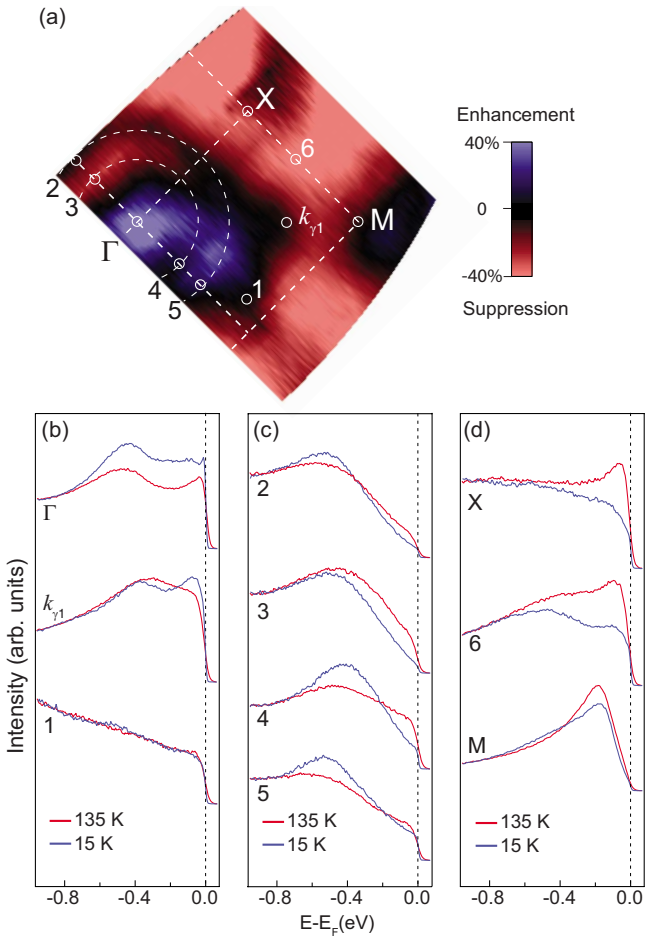

FIG. 3. (Color online) (a) The difference between the integrated spectral weight in 135 and 15 K over the $[E_F-0.7\ \text{eV}, E_F+0.05\ \text{eV}]$ window for $Fe_{1.06}Te$. (b)–(d) Temperature dependence of EDCs at various momenta as marked in panel (a).

opening is observed in all cases of Figs. 3(b)–3(d).[13,20] Early DFT calculations have predicted strong nesting instabilities with incorrect nesting wave vectors along the Γ-M direction.[7] Later on, it has been amended that the excess iron would significantly alter the electronic structure and produce the right wave vector.[25,26] However, this is ruled out by the absence of gap observed here.

Detailed temperature evolution of the spectral weight redistribution near T_s is shown in Fig. 4. The suppression at k_β occurs abruptly below T_s, and saturates at low temperatures [Fig. 4(a)]. Similar behavior takes place at k'_β [Fig. 4(a)] where the emergence of coherent quasiparticle could be clearly resolved. Furthermore, the temperature cycling experiment with dense steps around T_s in Fig. 4(b) gives a hysteresis loop in the integrated spectral weight in the Fig. 4(c). The hysteresis loop indicates a first-order phase transition character, similar to the susceptibility data in Fig. 4(d). This establishes a direct relation between the suppression and the SDW transition, which proves that our data reflect intrinsic and bulk properties. Note that the difference between k_β and k'_β might be caused by different k_z's or matrix element effects.

The high quality of the $Fe_{1.06}Te$ crystals studied here is shown by the narrow transitions in the resistivity [Fig. 1(e)]

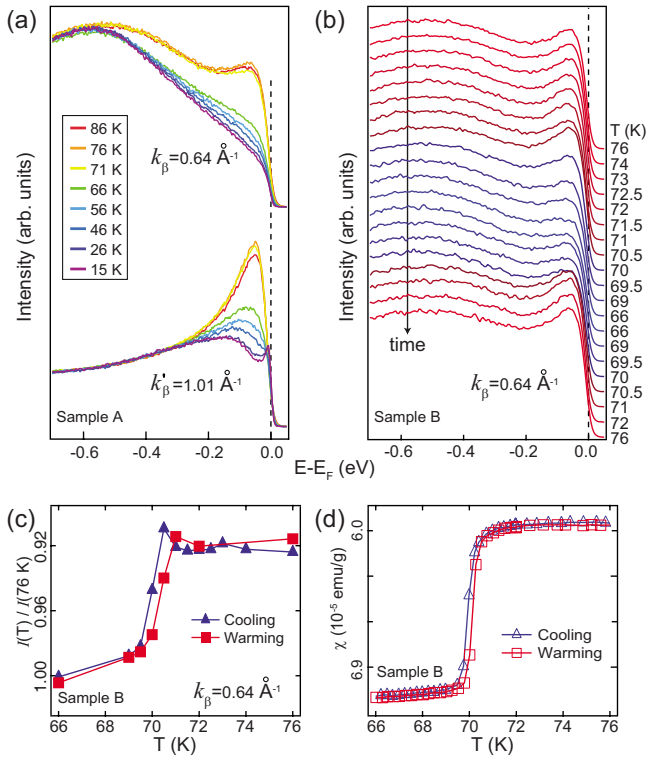

FIG. 4. (Color online) (a) Detailed temperature dependence of EDCs at the Fermi crossings of k_β and k'_β for sample A. (b) The EDC at k_β for sample B in a detailed temperature cycling experiment near T_s. (c) The integrated spectral weight over $[E_F-0.7$ eV, $E_F+0.05$ eV] as a function of temperature for data in panel (b), data are normalized by the integrated weight at 76 K. (d) The magnetic-susceptibility hysteresis loop. The sample A and B label the two samples that come from the same batch of single crystal $Fe_{1.06}Te$.

and magnetic-susceptibility data [Fig. 4(d)]. The sharp quasiparticles observed at low temperatures could further confirm that there is little scattering from the imperfection and impurities of the samples. More importantly, the observed spectral weight shows strong temperature dependence over a large energy scale, and the massive spectral weight distribution exhibit a hysteresis loop, similar to the bulk susceptibility data, which clearly prove that the broad features are *intrinsic* to $Fe_{1.06}Te$, as scattering from the defects or impurities should not exhibit much temperature dependence. Actually, there are no known extrinsic effects that would cause such a huge temperature dependence associated with the SDW. In addition, to show that such broad feature is not related to the excess Fe ions, the well-defined band structure of $Fe_{1.04}Te_{0.66}Se_{0.34}$ is shown in Fig. 2(g), where similar amount of interstitial Fe ions exist, except that the SDW is suppressed by the heavy Se doping. The low-temperature quasiparticle peak width of $Fe_{1.06}Te$ is even sharper than that of $Fe_{1.04}Te_{0.66}Se_{0.34}$ [Fig. 2(h)].

Our observation of the intrinsically broad electronic structure of $Fe_{1.06}Te$ and the spectral weight redistribution associated with SDW transition suggests strong local magnetic fluctuations and their strong coupling to itinerant electrons. Consequently, carriers are more localized, causing local moments and insulating transport behavior,[13] and coherent quasiparticles are destroyed in the paramagnetic states. However, in the SDW state, when the spin fluctuations are suppressed due to the opening of a spin gap as demonstrated by inelastic neutron scattering,[27] the sharp quasiparticles emerge. Consistently, it is found that the ordered moment in $Fe_{1+y}Te$ is about 2 μ_B,[12] much larger than the 0.87 μ_B in $BaFe_2As_2$, or the 0.36 μ_B in LaOFeAs.[9,10] Theoretically, the models based on magnetic exchange interactions between the nearest- and next-nearest-neighbor iron moments have successfully explained the bicollinear magnetic structure in $Fe_{1+y}Te$.[28,29] Our data will be a decisive support, if broad spectral function and related spectral weight redistribution can be reproduced in these models.

Furthermore, an early ARPES experiment[20] has shown that $Fe_{1.05}Te$ (T_s=65 K) exhibits an electronic structure close to that of the nonmagnetic $Fe_{1.04}Te_{0.66}Se_{0.34}$,[22] with more coherent electronic structure. No change in spectra has been observed through the SDW transition there. Since the magnetic order in iron chalcogenides could be strongly suppressed by just a small amount of Se, excess iron, or pressure,[14,30,31] our samples with higher T_s of 70 K are in a more strongly ordered state. It is remarkable to observe that the strong correlation effect is enhanced so dramatically here while T_s is just slightly increased. It is sensible to study how the correlations in iron-based systems are affected by anions (P/As/Se/Te), doping, and pressure.

In charge-density wave (CDW) systems such as 2H-TaS_2, strong electron-phonon interactions cause incoherent polaronic spectral line shape, and spectral weight at the E_F over the entire Brillouin zone. It was found that the massive spectral weight suppression over a large momentum and energy phase space, instead of Fermi-surface nesting, is responsible for the CDW in 2H-TaS_2 and 2H-$NbSe_2$.[32,33] The analogous mechanism of SDW found here for $Fe_{1.06}Te$ indicates the density waves at the strong-coupling limit share a universal theme, which makes them fundamentally different from the weak interaction systems.

IV. CONCLUSION

To summarize, we have carried out a systematic photoemission investigation of high-quality α-$Fe_{1.06}Te$ single crystals. We observed an intrinsically broad electronic structure, and massive spectral weight redistribution, which could drive the SDW from the electronic-structure perspective. Our results demonstrate that correlations are probably the strongest in $Fe_{1+y}Te$ among all Fe-HTSCs and their parent compounds discovered so far, and reveal universal behaviors of density waves in the presence of strong interactions.

ACKNOWLEDGMENTS

We thank Donghui Lu for helpful discussions. This work was supported by the NSFC, MOE, MOST (National Basic Research Program No. 2006CB921300), and STCSM of China.

*dlfeng@fudan.edu.cn

[1] Y. Kamihara, T. Watanabe, M. Hirano, and H. Hosono, J. Am. Chem. Soc. **130**, 3296 (2008).

[2] X. H. Chen, T. Wu, G. Wu, R. H. Liu, H. Chen, and D. F. Fang, Nature (London) **453**, 761 (2008).

[3] M. Rotter, M. Tegel, and D. Johrendt, Phys. Rev. Lett. **101**, 107006 (2008).

[4] K.-W. Yeh, T.-W. Huang, Y.-l. Huang, T.-K. Chen, F.-C. Hsu, P. M. Wu, Y.-C. Lee, Y.-Y. Chu, C.-L. Chen, J.-Y. Luo, D.-C. Yan, and M.-K. Wu, EPL **84**, 37002 (2008).

[5] F.-C. Hsu, J.-Y. Luo, K.-W. Yeh, T.-K. Chen, T.-W. Huang, P.-M. Wu, Y.-C. Lee, Y.-L. Huang, Y.-Y. Chu, D.-C. Yan, and M.-K. Wu, Proc. Natl. Acad. Sci. U.S.A. **105**, 14262 (2008).

[6] S. Margadonna, Y. Takabayashi, Y. Ohishi, Y. Mizuguchi, Y. Takano, T. Kagayama, T. Nakagawa, M. Takata, and K. Prassides, Phys. Rev. B **80**, 064506 (2009).

[7] A. Subedi, L. Zhang, D. J. Singh, and M. H. Du, Phys. Rev. B **78**, 134514 (2008).

[8] D. J. Singh, Phys. Rev. B **78**, 094511 (2008).

[9] C. de la Cruz, Q. Huang, J. W. Lynn, J. Li, W. Ratcliff II, J. L. Zarestky, H. A. Mook, G. F. Chen, J. L. Luo, N. L. Wang, and P. Dai, Nature (London) **453**, 899 (2008).

[10] Q. Huang, Y. Qiu, W. Bao, M. A. Green, J. W. Lynn, Y. C. Gasparovic, T. Wu, G. Wu, and X. H. Chen, Phys. Rev. Lett. **101**, 257003 (2008).

[11] W. Bao, Y. Qiu, Q. Huang, M. A. Green, P. Zajdel, M. R. Fitzsimmons, M. Zhernenkov, S. Chang, M. Fang, B. Qian, E. K. Vehstedt, J. Yang, H. M. Pham, L. Spinu, and Z. Q. Mao, Phys. Rev. Lett. **102**, 247001 (2009).

[12] S. Li, C. de la Cruz, Q. Huang, Y. Chen, J. W. Lynn, J. Hu, Y.-L. Huang, F.-C. Hsu, K.-W. Yeh, M.-K. Wu, and P. Dai, Phys. Rev. B **79**, 054503 (2009).

[13] G. F. Chen, Z. G. Chen, J. Dong, W. Z. Hu, G. Li, X. D. Zhang, P. Zheng, J. L. Luo, and N. L. Wang, Phys. Rev. B **79**, 140509(R) (2009).

[14] T. J. Liu, X. Ke, B. Qian, J. Hu, D. Fobes, E. K. Vehstedt, H. Pham, J. H. Yang, M. H. Fang, L. Spinu, P. Schiffer, Y. Liu, and Z. Q. Mao, Phys. Rev. B **80**, 174509 (2009).

[15] L. X. Yang, Y. Zhang, H. W. Ou, J. F. Zhao, D. W. Shen, B. Zhou, J. Wei, F. Chen, M. Xu, C. He, Y. Chen, Z. D. Wang, X. F. Wang, T. Wu, G. Wu, X. H. Chen, M. Arita, K. Shimada, M. Taniguchi, Z. Y. Lu, T. Xiang, and D. L. Feng, Phys. Rev. Lett. **102**, 107002 (2009).

[16] Y. Zhang, J. Wei, H. W. Ou, J. F. Zhao, B. Zhou, F. Chen, M. Xu, C. He, G. Wu, H. Chen, M. Arita, K. Shimada, H. Namatame, M. Taniguchi, X. H. Chen, and D. L. Feng, Phys. Rev. Lett. **102**, 127003 (2009).

[17] M. Yi, D. H. Lu, J. G. Analytis, J.-H. Chu, S.-K. Mo, R.-H. He, M. Hashimoto, R. G. Moore, I. I. Mazin, D. J. Singh, Z. Hussain, I. R. Fisher, and Z.-X. Shen, Phys. Rev. B **80**, 174510 (2009).

[18] C. He, Y. Zhang, B. P. Xie, X. F. Wang, L. X. Yang, B. Zhou, F. Chen, M. Arita, K. Shimada, H. Namatame, M. Taniguchi, X. H. Chen, J. P. Hu, and D. L. Feng, Phys. Rev. Lett. **105**, 117002 (2010).

[19] J. Dong, H. J. Zhang, G. Xu, Z. Li, G. Li, W. Z. Hu, D. Wu, G. F. Chen, X. Dai, J. L. Luo, Z. Fang, and N. L. Wang, EPL **83**, 27006 (2008).

[20] Y. Xia, D. Qian, L. Wray, D. Hsieh, G. F. Chen, J. L. Luo, N. L. Wang, and M. Z. Hasan, Phys. Rev. Lett. **103**, 037002 (2009).

[21] T. Taen, Y. Tsuchiya, Y. Nakajima, and T. Tamegai, Phys. Rev. B **80**, 092502 (2009).

[22] F. Chen, B. Zhou, Y. Zhang, J. Wei, H.-W. Ou, J.-F. Zhao, C. He, Q.-Q. Ge, M. Arita, K. Shimada, H. Namatame, M. Taniguchi, Z.-Y. Lu, J. Hu, X.-Y. Cui, and D. L. Feng, Phys. Rev. B **81**, 014526 (2010).

[23] A. Damascelli, Z. Hussain, and Z.-X. Shen, Rev. Mod. Phys. **75**, 473 (2003).

[24] A. Georges, G. Kotliar, W. Krauth, and M. J. Rozenberg, Rev. Mod. Phys. **68**, 13 (1996). Usually, one could consider a feature to be incoherent when its width is much larger than its centroid position from E_F.

[25] L. Zhang, D. J. Singh, and M. H. Du, Phys. Rev. B **79**, 012506 (2009).

[26] M. J. Han and S. Y. Savrasov, Phys. Rev. Lett. **103**, 067001 (2009).

[27] J. Zhao, D.-X. Yao, S. Li, T. Hong, Y. Chen, S. Chang, W. Ratcliff, J. W. Lynn, H. A. Mook, G. F. Chen, J. L. Luo, N. L. Wang, E. W. Carlson, J. Hu, and P. Dai, Phys. Rev. Lett. **101**, 167203 (2008).

[28] C. Fang, B. A. Bernevig, and J. Hu, EPL **86**, 67005 (2009).

[29] F. Ma, W. Ji, J. Hu, Z.-Y. Lu, and T. Xiang, Phys. Rev. Lett. **102**, 177003 (2009).

[30] H. Okada, H. Takahashi, Y. Mizuguchi, Y. Takano, and H. Takahashi, J. Phys. Soc. Jpn. **78**, 083709 (2009).

[31] P. L. Paulose, C. S. Yadav, and K. M. Subhedar, EPL **90**, 27011 (2010).

[32] D. W. Shen, B. P. Xie, J. F. Zhao, L. X. Yang, L. Fang, J. Shi, R. H. He, D. H. Lu, H. H. Wen, and D. L. Feng, Phys. Rev. Lett. **99**, 216404 (2007).

[33] D. W. Shen, Y. Zhang, L. X. Yang, J. Wei, H. W. Ou, J. K. Dong, B. P. Xie, C. He, J. F. Zhao, B. Zhou, M. Arita, K. Shimada, H. Namatame, M. Taniguchi, J. Shi, and D. L. Feng, Phys. Rev. Lett. **101**, 226406 (2008).